



A Journal of



Accepted Article

Title: Phosphines with N-heterocyclic Boryl-substituents: Ligands for Coordination Chemistry and Catalysis

Authors: Manuel Kaaz, Ralf J C Locke, Luisa Merz, Mathis Benedikter, Simon König, Johannes Bender, Simon H Schlindwein, Martin Nieger, and Dietrich Gudat

This manuscript has been accepted after peer review and appears as an Accepted Article online prior to editing, proofing, and formal publication of the final Version of Record (VoR). This work is currently citable by using the Digital Object Identifier (DOI) given below. The VoR will be published online in Early View as soon as possible and may be different to this Accepted Article as a result of editing. Readers should obtain the VoR from the journal website shown below when it is published to ensure accuracy of information. The authors are responsible for the content of this Accepted Article.

To be cited as: *Eur. J. Inorg. Chem.* 10.1002/ejic.201801081

Link to VoR: <http://dx.doi.org/10.1002/ejic.201801081>

WILEY-VCH

Phosphines with N-heterocyclic Boryl-substituents: Ligands for Coordination Chemistry and Catalysis

Manuel Kaaz,^[a] Ralf J. C. Locke,^[a] Luisa Merz,^[a] Mathis Benedikter,^[a] Simon König,^[a] Johannes Bender,^[a] Simon H. Schlindwein,^[a] Martin Nieger,^[b] and Dietrich Gudat^{*,[a]}

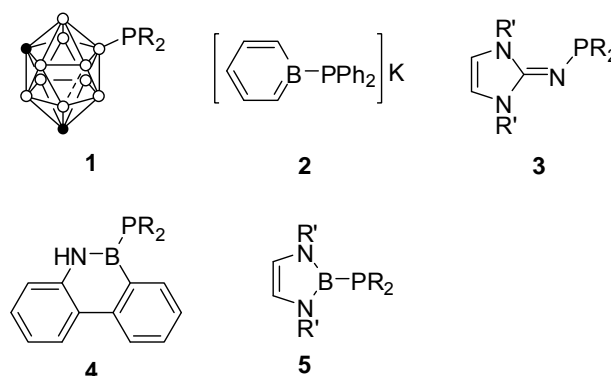
Dedicated to Professor Dr. Edgar Niecke on the occasion of his 80th and to Professor Dr. Koop Lammertsma on the occasion of his 70th birthday.

Abstract: Boryl-substituted phosphines NHB–P(R)Ph (R = H, Ph, NHB = N-heterocyclic boryl substituent) react with Fe₂(CO)₉ to give isolable Fe(CO)₄-complexes, two of which were characterized by single-crystal XRD studies. The electronic and steric properties for a series of the boryl phosphines were further assessed by evaluation of TEPs for in-situ formed complexes [RhCl(NHB–PR¹R²)(CO)₂] (R¹, R² = H, Ph, Me, NMe₂), and calculations of buried volumes for Fe(CO)₄-complexes. The results imply that the NHB-phosphines exhibit due to their conformational flexibility some variability in their steric bulk, and that some specimens may exhibit similar electron releasing power and steric demand as tBu₃P. Studies of the amination of bromobenzene with 2,6-diisopropylaniline confirmed that these properties can be exploited to promote Pd-catalyzed C–N cross coupling reactions, and that formal replacement of a phenyl by a NHB substituent in the auxiliary phosphine has a beneficial effect on catalyst performance.

Introduction

The usefulness of phosphines in coordination chemistry and catalysis is closely connected with the recognition that changing substituents on phosphorus can cause marked variations in the ligand behavior, which offer in turn options to manipulate the electron density and steric accessibility of the metal center of transition metal complexes with these ligands.^[1] This flexibility is of particular importance during the adaptation and optimization of catalytic processes. A lucid example is the amination of aryl halides with palladium phosphine complexes as catalysts that is known as Buchwald-Hartwig coupling.^{[3],[4]} The consequent elaboration of phosphine ligands with high electron donating power and steric demand permitted extending its scope to enable reactions under activation of difficult substrates, at ambient temperature, or with very low catalyst loadings.^{[4],[5]} The phosphorus substituents employed to advance the electron donating power and steric bulk of phosphines include in most

cases alkyl and aryl groups.^[6] More recently, also heteroatom-based substituents have moved into focus. For example, Buchwald et al. discovered carboranyl-phosphines **1** (Scheme 1) which were considered more electron rich than any other known alkyl- or aryl-based phosphine.^[6] Fu et al. described an anionic boratabenzene-phosphide **2** which was found to be a more strongly donating ligand than isosteric PPh₃.^[7] The groups of Kuhn^[8] and Dielmann^[9] drew on bulky imidazolin-2-ylideneimino-units^[10] to create phosphines **3**.^[11] These species display a similar electron donating ability as N-heterocyclic carbenes (NHCs) which enables them to promote the Suzuki-Miyaura cross-coupling of aryl chlorides with boronic acid, or to form isolable adducts with CO₂,^[12] respectively. The high electron donating power of **1** - **3** was inferred from structural and spectroscopic studies and related to the strongly π -donating character of the guanidinato substituent and the electron releasing properties of the anionic boratabenzene unit or the B-bound carborane cage, respectively.^{[6],[7],[9]} Pringle et al. reported that an increase in the electron donating power of phosphine ligands was likewise observable upon formal replacement of aryl units by isoelectronic B-based aminoboranyl substituents, and that a rhodium complex of **4** showed higher catalytic activity in the hydrogenation of cyclohexene than the complex containing an isoelectronic PCC-based phosphine.^[13] These findings imply that the idea to employ boryl substituents on phosphorus for boosting the electron donating power of phosphines, which had first been expressed in case of **1**, is presumably more widely applicable.



Scheme 1. Examples of P-heteroatom substituted electron rich phosphines (R, R' = alkyl, aryl); open and closed circles in the structure of **1** denote B- and C-centered vertices of a carboranyl (meta-C₂B₁₀H₁₁) substituent.

[a] M. Kaaz, L. Merz, M. Benedikter, S. König, J. Bender, S. H. Schlindwein, Prof. Dr. Dr. h. c. D. Gudat
Institut für Anorganische Chemie, University of Stuttgart,
Pfaffenwaldring 55, 70550 Stuttgart, Germany
E-mail: gudat@iac.uni-stuttgart.de
http://www.iac.uni-stuttgart.de/arbeitskreise/akgudat

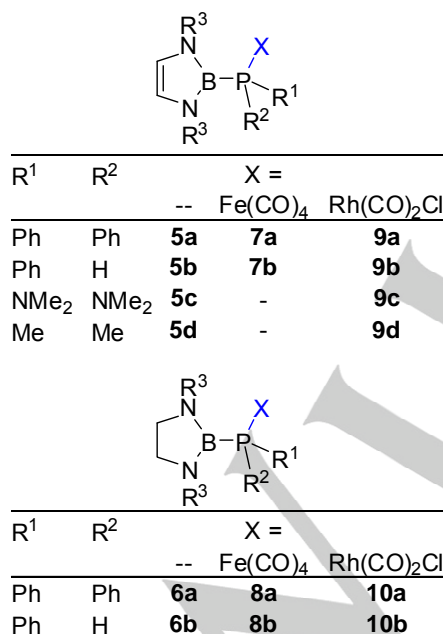
[b] Dr. M. Nieger
Department of Chemistry,
University of Helsinki
P.O. Box 55, 00014 University of Helsinki, Finland

Supporting information for this article is given via a link at the end of the document.

Some time ago, we had described the phosphines **5** (Scheme 1) with N-heterocyclic boryl substituents (NHB-phosphines) and noted that these molecules lack a significant boron-centered electrophilic character but may potentially bind to metal centers through their phosphorus atom.^[14] Considering that the NHB fragment embodies, like an alkyl group, essentially a strong σ -donor substituent, the phosphines **5** may be regarded as electron rich, strongly electron donating ligands. Starting from this hypothesis, we initiated a study of the metal coordination properties of these NHB-substituted phosphines. Herein, we report on the formation of isolable metal complexes, a study of the steric and electronic ligand properties, and a first application as electron rich ligand in a catalytic Buchwald-Hartwig reaction.

Results and Discussion

The studies described in this work were performed using NHB-phosphines carrying both CC-unsaturated 1,3,2-diazaborolyl substituents (**5a-d**, Scheme 2) and CC-saturated 1,3,2-diazaborolidinyl substituents (**6a,b**) on phosphorus. Ligands **5a-c**^[14] and **6a,b**^[15] had been reported previously and were synthesized as described. The P-alkyl derivative **5d** was newly prepared by analogy to **5a,b** from the appropriate 2-bromo-1,3,2-diazaborole and lithium dimethyl phosphide, and characterized by multinuclear NMR spectroscopy. Like its congeners,^{[14],[15]} the new NHB-phosphine is thermally stable in solution and the solid state, and can be shortly handled in air without decomposition.



Scheme 2. Molecular structures of NHB-substituted phosphines and their complexes included in this study (R³ = 2,6-iPr₂C₆H₃, Dipp).

Attempting to prepare isolable complexes with NHB-phosphine ligands, we established that **5a,b** and **6a,b** react smoothly with Fe₂(CO)₉ to give isolable iron pentacarbonyl and complexes **7a,b** and **8a,b**, which were unambiguously identified by their NMR and IR spectral data. Recrystallization from pentane produced single-crystals of complexes **7b** and **8b** which were further characterized by single-crystal X-ray diffraction studies. Attempts to produce single-crystals of **7a** and **8a** were as yet unsuccessful. The crystals **7b** and **8b** contain isolated molecular complexes (see Figure 1 for **7b**; the molecular structure of **8b**, and selected metrical parameters of both species and the ligands **5b** and **6b** are listed in Table S1 in the supporting information). Although the crystals are not isotopic, the molecular conformations and individual metrical parameters in both species are closely similar.

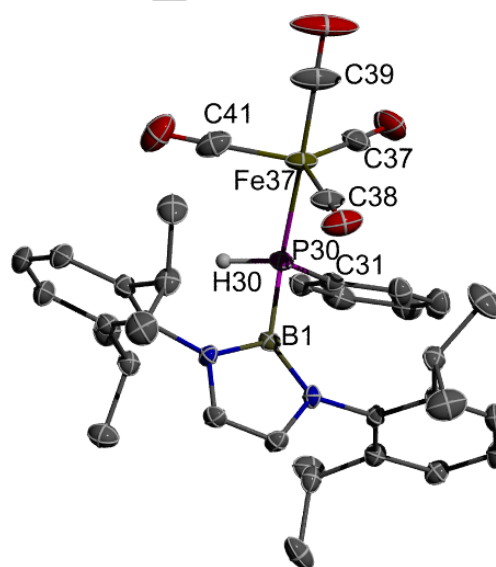


Figure 1. Molecular structure of **7b** in the crystal. Thermal ellipsoids are drawn at the 50% probability level and hydrogen atoms except H30 were omitted for clarity. Selected distances [Å] and angles [°]: B1-P30 1.948(2), P30-C31 1.822(2), P30-Fe37 2.2635(6), P30-H30 1.28(2), Fe37-C39 1.784(2), Fe37-C40 1.791(3), Fe37-C38 1.798(2), Fe37-C37 1.799(3), C31-P30-B1 108.50(9), C31-P30-H30 98.5(10), B1-P30-H30 97.3(10).

Interaction of the metal atoms with the carbon atoms of four carbonyls and the phosphorus atom of the NHB-phosphine gives rise to a trigonal-bipyramidal coordination geometry expected for Fe(0) centers with a formal d⁸ electron configuration. There is no indication for a η^2 -type interaction of the PB-unit with the metal atom, which had been observed for a phosphinoborane featuring a strongly electrophilic boryl substituent and high P–B double bond character.^[16] The phosphine ligands in **7b**, **8b** occupy axial coordination sites as in the majority of known phosphine-iron tetracarbonyl complexes.^[17] The Fe–P distances (**7b**: 2.264(1) Å, **8b**: 2.266(1) Å) lie slightly above the mean distance of 2.254(35) Å for known phosphine-Fe(CO)₄ complexes,^[17] but are in the normal range. The Fe–C distances are unexceptional.

Comparison of intra-ligand distances in **7b/8b** and the free ligands **5b/6b** (Table S1) reveals that the P–B bonds lengthen upon metal coordination whereas the P–C and P–H bonds display a slight shortening that is, however, on the verge of being not significant. The P–B bond lengthening is presumably attributable to the fact that the weak P→B π -bonding contribution in the free ligand^[14] is further cut back when the lone-pair on phosphorus gets involved in metal bonding. A further noteworthy difference between free and metal bound ligands in the crystal structures is a different alignment of the bulky NHB-moiety (Figure 2), which can be traced back to torsional twists of the heterocyclic ring and the N-aryl groups around the P–B and N–C bonds, respectively. This conformational reorientation reduces steric crowding in the vicinity of the metal centers and attests to a notable conformational flexibility of the NHB-phosphines.

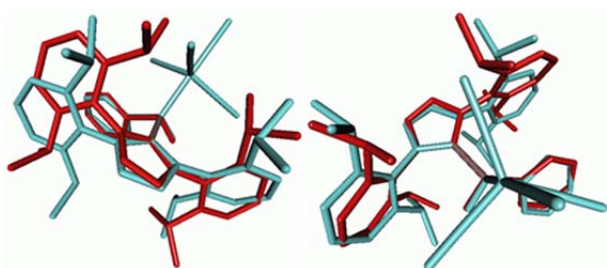


Figure 2. Overlay of the molecular structures of ligand **5b** (red, data from ref. [14]) and complex **7b** (light blue) viewed from two directions. Molecules are represented using a wire model, and all but the phosphorus-bound hydrogen atoms were omitted for clarity.

The molecular structures of **7b/8b** confirm the ability of the NHB-phosphines **5b/6b** to act as ligands in transition metal complexes, but the variations in individual bond distances and angles do not allow inferring a quantifiable picture of their donor properties. To this end, we turned to an analysis of trends in the "Tolman electronic parameter" (TEP)^[1] which remains, despite the development of alternative or more sophisticated descriptors or quantum chemically based concepts, still popular as a measure of the electron density a ligand L in a complex imparts on the metal center.^[18] For practical reasons, all studies were carried out on rhodium complexes [(L)RhCl(CO)₂] (L = **5a-d**, **6a,b**) which were generated in situ from reactions of the ligands with [(RhCl(cod))₂] and CO.^[19] The wavenumbers of the $\nu(\text{CO})$ modes derived from IR spectra were converted^[20] to the commonly used scale^[1] which refers to the wavenumbers of the totally symmetric $\nu(\text{CO})$ vibrational mode of the appropriate Ni(CO)₃ complexes.

The TEPs of all NHB-phosphines studied are similar or even larger than those of alkyl phosphines (Table 1), and the value for **5d** approaches even those reported for some NHCs. The net electron donating ability of all ligands but **5b/6b** may on this scale be rated to exceed that of P(*t*Bu)₃, the strongest all-carbon substituted phosphorus donor known so far. The depression of the TEP upon formal exchange of the phenyl in a phosphine R¹R²PhP by a NHB unit amounts to $\Delta\tilde{\nu} = 12\text{--}15\text{ cm}^{-1}$ and exceeds the shifts of 4.2 and 8.1 cm^{-1} induced by exchange of a

phenyl in PPh₃ by more electron releasing *t*Bu^[21] or 1,3-diisopropyl-benzimidazol-2-ylidenimino-moieties,^[9] respectively. In contrast, the presence (in **5a,b**) or absence (in **6a,b**) of a CC-double bond in the NHB unit has no visible effect on the TEP. In view of the general non-additivity of substituent contributions to the TEP^[22] and the variance of $\Delta\tilde{\nu}$, these results do not allow us to extract a quantifiable and transferable substituent increment which characterizes the influence of NHB-units on the electron donor properties a phosphine. Nonetheless, they confirm qualitatively that the NHB substituent can, like a *m*-carboranyl moiety,^[6] boost its net electron donating power beyond the range accessible for phosphines with only carbon-based substituents.

Table 1. Values of TEP and %V_{bur} for NHB-phosphines **5a-d**, **6a,b** and selected reference compounds.

Ligand	TEP [cm^{-1}]	%V _{bur}
5a	2055.5	-- (37)
6a	2054.9	-- (38)
5b	2058.4	27 (32)
6b	2058.2	29 (32)
5c	2053.7	-- (39)
5d	2052.8	-- (30)
PPh ₃	2068.9 ^[d]	29
PPh ₂ H	2073.3 ^[d]	25
PPh(NMe ₂) ₂	2065.6 ^[e]	--
PPhMe ₂	2065.3 ^[d]	25
P(<i>t</i> Bu) ₃	2056.1 ^[d]	34
SIMes ^[a]	2052.0 ^[f]	32
IMes ^[b]	2050.8 ^[f]	32
<i>t</i> Bu ^[b]	2050.1 ^[f]	35 ^[h]
P(NB <i>i</i> Pr)Ph ₂ ^[c]	2060.8 ^[g]	40 ^[g]

[a] SIMes = 1,3-dimesityl-imidazol-2-ylidene. [b] IMes/*t*Bu = 1,3-dimesityl/*di-t*-butyl-imidazol-2-ylidene. [c] NB*i*Pr = 1,3-diisopropyl-benzimidazol-2-ylidenimino. [d] data from ref. [1]. [e] data from ref. [22]. [f] data from ref. [20]. [g] data from ref. [9]. [h] data for [(C₅H₃*t*Bu₂)Fe(P(*t*Bu)₃)] as the crystal structure of the Fe(CO)₄ complex is unknown.

The steric properties of phosphines are often assessed via their cone angle.^[1] However, the use of this descriptor, which goes likewise back to the work of Tolman, faces known limitations when the shape of a ligand cannot be well approximated by a cone.^[23] In view of the irregular shape of the NHB-phosphines **5**, **6**, we presumed that analysis of the percent buried volume %V_{bur}^[24] can provide a more logical and realistic picture of trends in steric properties. This descriptor was developed for analyzing

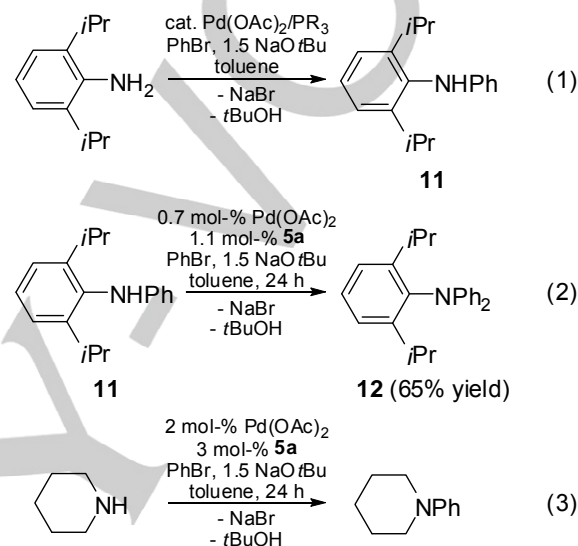
the sterics of NHCs, but is also routinely applied to other types of ligands. Computation of $\%V_{bur}$ is in principle feasible on the basis of both crystal structure data and molecular geometries from quantum chemical calculations, but requires a careful choice of the data source employed to model the ligand geometry.^{[20][24]} In particular, using structural data of a free ligand and its metal complex can yield quite different results when the metal coordination goes along with a conformational change that alters the overall ligand shape. As this is the case for the NHB-phosphines, we refrained from analyzing the structures of the free ligands (even if a complete set of crystal structure data is available). Instead, we computed buried volumes for **5b**, **6b** and selected reference compounds using the crystal structure data of the iron complexes **7b**, **8b** and published crystallographic data of appropriate $\text{Fe}(\text{CO})_4$ complexes in the CSD^[17] as input. In addition, we computed buried volumes for all NHB-phosphines using energy optimized geometries obtained from DFT-calculations (see experimental section and supporting information for details). All results are collected in Table 1.

The buried volumes of ligands **5b**, **6b** in the complexes **7b**, **8b** compare to that of PPh_3 in $[\text{Fe}(\text{PPh}_3)(\text{CO})_4]$ but are clearly smaller than the values derived with DFT-calculated molecular geometries. This discrepancy can be traced to the presence of visibly different ligand conformations in calculated and observed structures of **7b**, **8b**. Since the calculations reproduce bond distances and angles quite well, we explain this deviation as reflecting mainly the impact of packing effects in the crystal, and rate it as a further proof for the conformational flexibility of the ligands. That the steric demand inferred from $\%V_{bur}$ -values can be viewed as snapshot which may not fully account for the flexibility of a ligand (with the implication that values computed for different complexes with the same ligand, or even different conformers of a complex, may be subject to sizable variation) had been pointed out earlier.^[20]

Comparison of buried volumes of all ligands **5a-d/6a,b** derived from DFT-optimized molecular geometries for complexes **7a-d/8a,b** confirms the expected increase in steric bulk upon formal replacement of the PhHPH -fragment by PPh_2 - or $\text{P}(\text{NMe}_2)_2$ -units, respectively. In contrast, formal exchange of the PHPH - by a PMe_2 -moiety has practically no effect. In view of the sensitivity of the buried volume toward conformational changes^[20] and metal-ligand distances,^[24] we consider the small variations between phosphines with unsaturated (**5a,b**) and saturated (**6a,b**) NHB rings insignificant and refrain from an interpretation. In comparison to other phosphines and NHCs (Table 1), the steric bulk of **5b/6b** is rated as similar to that of PPh_3 , whereas **5d** should be assessed as slightly smaller. The overall steric bulk of **5a,d** and **6a** may be considered as roughly comparable to that of $\text{P}(\text{tBu})_3$ and *N*-mesityl substituted NHCs but does not reach that of bulky Buchwald-type phosphines.^[25]

The electronic and steric descriptors listed in Table 1 suggest to rate NHB-phosphines as ligands that may impart high electron density and steric shielding to the metal center in a complex. As these characteristics are also essential prerequisites for active catalysts in Pd-catalyzed cross-coupling reactions,^[5] NHB-phosphines make promising candidates for application in cross-coupling catalysis. The best performance is expected for **5b/6b**

and **5c**, which excel the other NHB-phosphines in both electron releasing power and steric bulk. For a proof of principle, we performed an exemplary study of the Pd-catalyzed Buchwald-Hartwig coupling of bromobenzene with 2,6-diisopropylaniline (Dipp-NH_2) in refluxing toluene (reaction (1), Scheme 3). The reaction protocol copies a known synthesis of target amine **11** using a bulky Buchwald-type phosphine as activating ligand.^{[26][27]} For our studies, phosphine **5a** was deemed to provide the best compromise between optimum ligand properties, chemical stability, and easy synthetic accessibility.



Scheme 3. Pd-catalyzed aminations of bromobenzene studied in this work. Further details on the conditions for reaction (1) are given in Table 2.

Table 2. The effect of different reaction conditions on the amination of bromobenzene with 2,6-diisopropylaniline.

Entry	$n(\text{Pd}(\text{OAc})_2)$	Phosphine	Conditions	Conversion ^[a]
1	2 mol-%	3 mol-% 5a	2 h, 115 °C	100(72)% ^[b]
2	2 mol-%	3 mol-% PPh_3	2 h, 115 °C	100%
3	0.2 mol-%	0.3 mol-% 5a	2 h, 115 °C	100%
4	0.2 mol-%	0.3 mol-% PPh_3	3 h, 115 °C	100%
5 ^[c]	2 mol-%	3 mol-% 5a	10 min, 200 °C	100%
6 ^[c]	--	--	40 min, 270 °C	67%

[a] determined spectroscopically in the crude reaction product. [b] isolated yield after column chromatography in parentheses. [c] Reaction performed in a closed vessel under microwave irradiation.

Performing the reaction with the reported^[26] catalyst load (2 mol-% Pd(OAc)₂ and 3 mol-% phosphine) led to quantitative conversion of the aryl halide within two hours. Work-up afforded the product in a yield 72% (Table 2, entry 1), which is slightly smaller than the reported yield of 82% after 8 hours reaction using a Buchwald-type phosphine. Unexpectedly, we found that quantitative conversion is also achieved when PPh₃ instead of **5a** is used as activating ligand (Table 2, entry 2), indicating that the use of tailored phosphines is not essential in this particular case. Presuming that the seemingly equal performance of **5a** and PPh₃ arises from an overloading with catalyst, we repeated the reactions with a reduced catalyst load (0.2 mol-% Pd(OAc)₂ and 0.3 mol-% phosphine) under otherwise identical conditions. Full conversion of the aryl halide was still feasible within two hours with **5a** (Table 2, entry 3) and three hours with PPh₃ (Table 2, entry 4). The different efficacy of the two phosphines was established by a kinetic study which disclosed that the activity of the catalyst based on **5a** (TOF = 7.0(4)·10³ h⁻¹) exceeds that of the PPh₃-based system (TOF = 2.83(3)·10³ h⁻¹) by a factor of 2.5 (Figure 3).

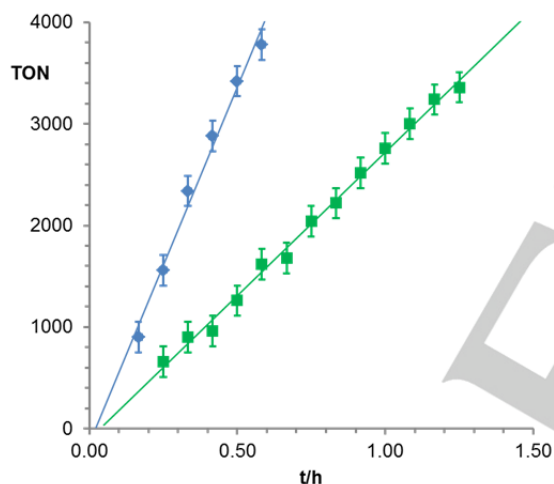


Figure 3. Plot of turnover numbers (TON = $n(\mathbf{11})/n(\text{Pd})$) during the early reaction stages vs. overall time for reaction (1) in Scheme 2. Blue diamonds (♦) refer to reactions carried out using **5a** and green squares (■) to reactions carried out using PPh₃ as auxiliary ligand, respectively. The straight lines represent the result of linear fits to the data. Turnover frequencies (TOF) of were obtained from the slopes of the regression lines.

Expectedly, NHB-phosphine **5a** promotes also the amination of iodobenzene with Dipp-NH₂ (quantitative conversion within <30 min), while no activity at all was observed with fluoro- or chlorobenzene as substrates. The efficacy of **5a** in syntheses of tertiary amines is illustrated in the coupling of bromobenzene with **11** (reaction (2)) and piperidine (reaction (3)); both reactions mimic reported syntheses with Buchwald-type ligands as auxiliary.^[26] Because conducting C–N cross-coupling reactions under microwave (MW) irradiation enables substantial time savings,^{[26][28]} we studied the synthesis of **11** in a MW reactor. Interestingly, quantitative reaction occurred within 10 min at 200 °C in the presence of Pd(OAc)₂ and **5a** as pre-catalysts

(entry 5 in Table 2), but 67% conversion to **11** was also achieved when the reaction was carried out under more forcing conditions (40 min at 270 °C; entry 6 in Table 2) in the absence of both Pd(OAc)₂ and **5a**. No reaction at all was observed at room temperature, either with or without catalyst. Transition metal-free, MW-assisted amination of aryl halides has previously been observed in other cases and was successfully incorporated in amine syntheses,^[29] but needs in the present case further elaboration of reaction conditions before it can compete with the Pd-catalyzed variant.

Conclusions

The reactions of NHB-phosphines with Fe₂(CO)₉ yield isolable complexes which were spectroscopically identified and in two cases fully characterized. The crystal structure data confirm that the NHB-phosphines act, like most previously known boryl phosphines,^[30] as P-donor ligands. The net electron donor capability, judged by the TEP, can be considered to match or even exceed that of highly electron rich trialkyl phosphines, including PtBu₃. Comparisons between observed and computed molecular structures of free NHB-phosphines and their iron complexes suggest that the NHB-substituents exhibit some conformational flexibility which can modulate the steric bulk of the ligand. Even if this effect encumbers a precise assessment, analysis of buried volumes for a series of Fe(CO)₄-complexes suggests that the steric bulk of NHB-phosphines is, depending on the ancillary P-substituents, comparable to that of common phosphines like PPh₃ or PtBu₃. The combination of strong electron releasing power and appreciable bulk makes NHB-phosphines appealing ligands for application in Pd-catalyzed cross-coupling reactions. An exemplary evaluation of Buchwald-Hartwig aminations of bromobenzene reveals that formal Ph/NHB-exchange in the auxiliary phosphine used has a definite accelerating effect, even if the performance of the ligand employed remains still lower than that of PtBu₃ which also promotes C–N cross-coupling at ambient temperature or with chlorobenzene as substrate.^[5] Nonetheless, NHB-phosphines with two bulky alkyl substituents or more than a single NHB-unit on phosphorus promise a further increase in both electron donor power and steric bulk and make thus interesting targets for further research.

Experimental Section

General Conditions: All manipulations were carried out under dry argon using Schlenk glassware. Solvents were purified and dried by standard methods. Microwave syntheses were carried out using an Anton Paar Monowave 400 reactor. NMR spectra: Bruker Avance 250 (¹H: 250 MHz, ¹¹B: 80.2 MHz, ¹³C: 62.9 MHz, ³¹P: 101.2 MHz) or Avance 400 (¹H: 400.13 MHz, ¹¹B: 128.3 MHz, ¹³C: 100.6 MHz, ³¹P: 162.9 MHz) in C₆D₆ or CDCl₃ at 30 °C. Chemical shifts were referenced to ext. TMS (¹H, ¹³C) using BF₃·OEt₂ (¹¹B, δ = 32.083974 MHz), or 85% H₃PO₄ (³¹P, δ = 40.480742 MHz) as secondary references. Coupling constants are given as absolute values. Elemental analyses: Elementar Micro Cube.

Synthesis of 5d: A solution of 2-bromo-1,3-bis(2,6-diisopropylphenyl)-1,3,2-diazaborole (2.00 g, 3.28 mmol) in THF (20 mL) was added at r.t. to a stirred solution of lithium dimethylphosphide (266 mg, 4.28 mmol) in THF (20 mL). The mixture was stirred for 16 h before all volatiles were evaporated under reduced pressure. The residue was dissolved in *n*-pentane (50 mL) and the suspension was filtered through celite. The filtrate was concentrated to a volume of 10 mL and stored at -20 °C to yield 1.30 g (2.90 mmol, 68%) of colorless crystals of **5d**. ¹H NMR (250 MHz, C₆D₆): δ = 6.98 (m, 6 H, C₆H₃), 6.04 (d, 2 H, ⁴J_{PH} = 0.8 Hz, NCH), 3.11 (sept, 4 H, ³J_{HH} = 6.9 Hz, CH(CH₃)₂), 1.14 (d, 12 H, ³J_{HH} = 6.9 Hz, CH(CH₃)₂), 1.00 (d, 12 H, ³J_{HH} = 6.9 Hz, CH(CH₃)₂), 0.54 (d, 6 H, ²J_{PH} = 1.7 Hz, PCH₃). ¹¹B NMR (128.3 MHz, C₆D₆): δ = 28.0 (br s). ¹³C{¹H} NMR (62.9 MHz, CDCl₃): δ = 146.1 (s, *o*-C₆H₃), 139.0 (s, *i*-C₆H₃), 127.4 (s, *p*-C₆H₃), 123.2 (s, *m*-C₆H₃), 120.9 (d, ³J_{PC} = 6.0 Hz, NCH), 28.4 (s, CH(CH₃)₂), 25.6 (s, CH(CH₃)₂), 23.1 (s, CH(CH₃)₂), 6.9 (d, ¹J_{PC} = 8.3 Hz, PCH₃). ³¹P-NMR (250 MHz, C₆D₆): δ = -120.9 (br s).

Synthesis of iron complexes: The appropriate NHB-phosphine (0.55 mmol) and Fe₂(CO)₉ (0.20 g, 0.55 mmol) were suspended in THF (10 mL) and the mixture was stirred for 10 h at ambient temperature. Filtration of the dark red solution formed through alumina produced a yellow solution which was once more evaporated to dryness. The residue was washed twice by suspension in pentane (5 mL) to produce a light yellow solution and a yellow solid. The supernatant liquid was subsequently removed with a syringe. Drying the residue under reduced pressure produced the products as yellow, microcrystalline powders (no yields determined).

7a: Yield 141 mg (198 μmol, 35%). ¹H NMR (400 MHz, CDCl₃): δ = 7.41 (m, 4 H, *o*-Ph), 7.18-7.07 (m, 6 H, *m/p*-Ph), 7.11 (t, 2 H, ³J_{HH} = 7.6 Hz, *p*-C₆H₃), 6.98 (d, 4 H, ³J_{HH} = 7.6 Hz, *m*-C₆H₃), 6.20 (d, 2 H, ⁴J_{PH} = 1.9 Hz, NCH), 3.04 (sept, 4 H, ³J_{HH} = 6.7 Hz, CH(CH₃)₂), 1.07 (d, 24 H, ³J_{HH} = 6.7 Hz, CH(CH₃)₂). ¹¹B NMR (128.3 MHz, CDCl₃): δ = 25.1 (br d, ¹J_{PB} = 108 Hz). ¹³C{¹H} NMR (62.9 MHz, CDCl₃): δ = 213.8 (d, ²J_{PC} = 18 Hz, CO) 145.7 (s, *i*-C₆H₃), 139.1 (s, *o*-C₆H₃), 134.5 (d, ²J_{PC} = 10.0 Hz, *o*-Ph), 130.0 (d, ⁴J_{PC} = 2.5 Hz, *p*-Ph), 128.5 (s, *p*-C₆H₃), 128.2 (d, ³J_{PC} = 10.2 Hz, *m*-Ph), 124.0 (d, ³J_{PC} = 6.3 Hz, NCH), 123.9 (s, *m*-C₆H₃), 29.3 (s, CH(CH₃)₂), 26.8 (s, CH(CH₃)₂). ³¹P-NMR (101.2, CDCl₃): δ = 8.08 (br d). ¹³C{¹H} NMR (62.9 MHz, CDCl₃): δ = 213.8 (d, ²J_{PC} = 18 Hz, CO) 145.7 (s, *i*-C₆H₃), 139.1 (s, *o*-C₆H₃), 134.5 (d, ²J_{PC} = 10.0 Hz, *o*-Ph), 130.0 (d, ⁴J_{PC} = 2.5 Hz, *p*-Ph), 128.5 (s, *p*-C₆H₃), 128.2 (d, ³J_{PC} = 10.2 Hz, *m*-Ph), 124.0 (d, ³J_{PC} = 6.3 Hz, NCH), 123.9 (s, *m*-C₆H₃), 29.3 (s, CH(CH₃)₂), 26.8 (s, CH(CH₃)₂). ³¹P-NMR (101.2, CDCl₃): δ = 8.08 (br d). ¹³C{¹H} NMR (62.9 MHz, CDCl₃): δ = 213.8 (d, ²J_{PC} = 18 Hz, CO) 145.7 (s, *i*-C₆H₃), 139.1 (s, *o*-C₆H₃), 134.5 (d, ²J_{PC} = 10.0 Hz, *o*-Ph), 130.0 (d, ⁴J_{PC} = 2.5 Hz, *p*-Ph), 128.5 (s, *p*-C₆H₃), 128.2 (d, ³J_{PC} = 10.2 Hz, *m*-Ph), 124.0 (d, ³J_{PC} = 6.3 Hz, NCH), 123.9 (s, *m*-C₆H₃), 29.3 (s, CH(CH₃)₂), 26.8 (s, CH(CH₃)₂). ³¹P-NMR (101.2, CDCl₃): δ = 8.08 (br d). ¹³C{¹H} NMR (62.9 MHz, CDCl₃): δ = 213.8 (d, ²J_{PC} = 18 Hz, CO) 145.7 (s, *i*-C₆H₃), 139.1 (s, *o*-C₆H₃), 134.5 (d, ²J_{PC} = 10.0 Hz, *o*-Ph), 130.0 (d, ⁴J_{PC} = 2.5 Hz, *p*-Ph), 128.5 (s, *p*-C₆H₃), 128.2 (d, ³J_{PC} = 10.2 Hz, *m*-Ph), 124.0 (d, ³J_{PC} = 6.3 Hz, NCH), 123.9 (s, *m*-C₆H₃), 29.3 (s, CH(CH₃)₂), 26.8 (s, CH(CH₃)₂). ³¹P-NMR (101.2, CDCl₃): δ = 8.08 (br d). ¹³C{¹H} NMR (62.9 MHz, CDCl₃): δ = 213.8 (d, ²J_{PC} = 18 Hz, CO) 145.7 (s, *i*-C₆H₃), 139.1 (s, *o*-C₆H₃), 134.5 (d, ²J_{PC} = 10.0 Hz, *o*-Ph), 130.0 (d, ⁴J_{PC} = 2.5 Hz, *p*-Ph), 128.5 (s, *p*-C₆H₃), 128.2 (d, ³J_{PC} = 10.2 Hz, *m*-Ph), 124.0 (d, ³J_{PC} = 6.3 Hz, NCH), 123.9 (s, *m*-C₆H₃), 29.3 (s, CH(CH₃)₂), 26.8 (s, CH(CH₃)₂). ³¹P-NMR (101.2, CDCl₃): δ = 8.08 (br d). ¹³C{¹H} NMR (62.9 MHz, CDCl₃): δ = 213.8 (d, ²J_{PC} = 18 Hz, CO) 145.7 (s, *i*-C₆H₃), 139.1 (s, *o*-C₆H₃), 134.5 (d, ²J_{PC} = 10.0 Hz, *o*-Ph), 130.0 (d, ⁴J_{PC} = 2.5 Hz, *p*-Ph), 128.5 (s, *p*-C₆H₃), 128.2 (d, ³J_{PC} = 10.2 Hz, *m*-Ph), 124.0 (d, ³J_{PC} = 6.3 Hz, NCH), 123.9 (s, *m*-C₆H₃), 29.3 (s, CH(CH₃)₂), 26.8 (s, CH(CH₃)₂). ³¹P-NMR (101.2, CDCl₃): δ = 8.08 (br d). ¹³C{¹H} NMR (62.9 MHz, CDCl₃): δ = 213.8 (d, ²J_{PC} = 18 Hz, CO) 145.7 (s, *i*-C₆H₃), 139.1 (s, *o*-C₆H₃), 134.5 (d, ²J_{PC} = 10.0 Hz, *o*-Ph), 130.0 (d, ⁴J_{PC} = 2.5 Hz, *p*-Ph), 128.5 (s, *p*-C₆H₃), 128.2 (d, ³J_{PC} = 10.2 Hz, *m*-Ph), 124.0 (d, ³J_{PC} = 6.3 Hz, NCH), 123.9 (s, *m*-C₆H₃), 29.3 (s, CH(CH₃)₂), 26.8 (s, CH(CH₃)₂). ³¹P-NMR (101.2, CDCl₃): δ = 8.08 (br d). ¹³C{¹H} NMR (62.9 MHz, CDCl₃): δ = 213.8 (d, ²J_{PC} = 18 Hz, CO) 145.7 (s, *i*-C₆H₃), 139.1 (s, *o*-C₆H₃), 134.5 (d, ²J_{PC} = 10.0 Hz, *o*-Ph), 130.0 (d, ⁴J_{PC} = 2.5 Hz, *p*-Ph), 128.5 (s, *p*-C₆H₃), 128.2 (d, ³J_{PC} = 10.2 Hz, *m*-Ph), 124.0 (d, ³J_{PC} = 6.3 Hz, NCH), 123.9 (s, *m*-C₆H₃), 29.3 (s, CH(CH₃)₂), 26.8 (s, CH(CH₃)₂). ³¹P-NMR (101.2, CDCl₃): δ = 8.08 (br d). ¹³C{¹H} NMR (62.9 MHz, CDCl₃): δ = 213.8 (d, ²J_{PC} = 18 Hz, CO) 145.7 (s, *i*-C₆H₃), 139.1 (s, *o*-C₆H₃), 134.5 (d, ²J_{PC} = 10.0 Hz, *o*-Ph), 130.0 (d, ⁴J_{PC} = 2.5 Hz, *p*-Ph), 128.5 (s, *p*-C₆H₃), 128.2 (d, ³J_{PC} = 10.2 Hz, *m*-Ph), 124.0 (d, ³J_{PC} = 6.3 Hz, NCH), 123.9 (s, *m*-C₆H₃), 29.3 (s, CH(CH₃)₂), 26.8 (s, CH(CH₃)₂). ³¹P-NMR (101.2, CDCl₃): δ = 8.08 (br d). ¹³C{¹H} NMR (62.9 MHz, CDCl₃): δ = 213.8 (d, ²J_{PC} = 18 Hz, CO) 145.7 (s, *i*-C₆H₃), 139.1 (s, *o*-C₆H₃), 134.5 (d, ²J_{PC} = 10.0 Hz, *o*-Ph), 130.0 (d, ⁴J_{PC} = 2.5 Hz, *p*-Ph), 128.5 (s, *p*-C₆H₃), 128.2 (d, ³J_{PC} = 10.2 Hz, *m*-Ph), 124.0 (d, ³J_{PC} = 6.3 Hz, NCH), 123.9 (s, *m*-C₆H₃), 29.3 (s, CH(CH₃)₂), 26.8 (s, CH(CH₃)₂). ³¹P-NMR (101.2, CDCl₃): δ = 8.08 (br d). ¹³C{¹H} NMR (62.9 MHz, CDCl₃): δ = 213.8 (d, ²J_{PC} = 18 Hz, CO) 145.7 (s, *i*-C₆H₃), 139.1 (s, *o*-C₆H₃), 134.5 (d, ²J_{PC} = 10.0 Hz, *o*-Ph), 130.0 (d, ⁴J_{PC} = 2.5 Hz, *p*-Ph), 128.5 (s, *p*-C₆H₃), 128.2 (d, ³J_{PC} = 10.2 Hz, *m*-Ph), 124.0 (d, ³J_{PC} = 6.3 Hz, NCH), 123.9 (s, *m*-C₆H₃), 29.3 (s, CH(CH₃)₂), 26.8 (s, CH(CH₃)₂). ³¹P-NMR (101.2, CDCl₃): δ = 8.08 (br d). ¹³C{¹H} NMR (62.9 MHz, CDCl₃): δ = 213.8 (d, ²J_{PC} = 18 Hz, CO) 145.7 (s, *i*-C₆H₃), 139.1 (s, *o*-C₆H₃), 134.5 (d, ²J_{PC} = 10.0 Hz, *o*-Ph), 130.0 (d, ⁴J_{PC} = 2.5 Hz, *p*-Ph), 128.5 (s, *p*-C₆H₃), 128.2 (d, ³J_{PC} = 10.2 Hz, *m*-Ph), 124.0 (d, ³J_{PC} = 6.3 Hz, NCH), 123.9 (s, *m*-C₆H₃), 29.3 (s, CH(CH₃)₂), 26.8 (s, CH(CH₃)₂). ³¹P-NMR (101.2, CDCl₃): δ = 8.08 (br d). ¹³C{¹H} NMR (62.9 MHz, CDCl₃): δ = 213.8 (d, ²J_{PC} = 18 Hz, CO) 145.7 (s, *i*-C₆H₃), 139.1 (s, *o*-C₆H₃), 134.5 (d, ²J_{PC} = 10.0 Hz, *o*-Ph), 130.0 (d, ⁴J_{PC} = 2.5 Hz, *p*-Ph), 128.5 (s, *p*-C₆H₃), 128.2 (d, ³J_{PC} = 10.2 Hz, *m*-Ph), 124.0 (d, ³J_{PC} = 6.3 Hz, NCH), 123.9 (s, *m*-C₆H₃), 29.3 (s, CH(CH₃)₂), 26.8 (s, CH(CH₃)₂). ³¹P-NMR (101.2, CDCl₃): δ = 8.08 (br d). ¹³C{¹H} NMR (62.9 MHz, CDCl₃): δ = 213.8 (d, ²J_{PC} = 18 Hz, CO) 145.7 (s, *i*-C₆H₃), 139.1 (s, *o*-C₆H₃), 134.5 (d, ²J_{PC} = 10.0 Hz, *o*-Ph), 130.0 (d, ⁴J_{PC} = 2.5 Hz, *p*-Ph), 128.5 (s, *p*-C₆H₃), 128.2 (d, ³J_{PC} = 10.2 Hz, *m*-Ph), 124.0 (d, ³J_{PC} = 6.3 Hz, NCH), 123.9 (s, *m*-C₆H₃), 29.3 (s, CH(CH₃)₂), 26.8 (s, CH(CH₃)₂). ³¹P-NMR (101.2, CDCl₃): δ = 8.08 (br d). ¹³C{¹H} NMR (62.9 MHz, CDCl₃): δ = 213.8 (d, ²J_{PC} = 18 Hz, CO) 145.7 (s, *i*-C₆H₃), 139.1 (s, *o*-C₆H₃), 134.5 (d, ²J_{PC} = 10.0 Hz, *o*-Ph), 130.0 (d, ⁴J_{PC} = 2.5 Hz, *p*-Ph), 128.5 (s, *p*-C₆H₃), 128.2 (d, ³J_{PC} = 10.2 Hz, *m*-Ph), 124.0 (d, ³J_{PC} = 6.3 Hz, NCH), 123.9 (s, *m*-C₆H₃), 29.3 (s, CH(CH₃)₂), 26.8 (s, CH(CH₃)₂). ³¹P-NMR (101.2, CDCl₃): δ = 8.08 (br d). ¹³C{¹H} NMR (62.9 MHz, CDCl₃): δ = 213.8 (d, ²J_{PC} = 18 Hz, CO) 145.7 (s, *i*-C₆H₃), 139.1 (s, *o*-C₆H₃), 134.5 (d, ²J_{PC} = 10.0 Hz, *o*-Ph), 130.0 (d, ⁴J_{PC} = 2.5 Hz, *p*-Ph), 128.5 (s, *p*-C₆H₃), 128.2 (d, ³J_{PC} = 10.2 Hz, *m*-Ph), 124.0 (d, ³J_{PC} = 6.3 Hz, NCH), 123.9 (s, *m*-C₆H₃), 29.3 (s, CH(CH₃)₂), 26.8 (s, CH(CH₃)₂). ³¹P-NMR (101.2, CDCl₃): δ = 8.08 (br d). ¹³C{¹H} NMR (62.9 MHz, CDCl₃): δ = 213.8 (d, ²J_{PC} = 18 Hz, CO) 145.7 (s, *i*-C₆H₃), 139.1 (s, *o*-C₆H₃), 134.5 (d, ²J_{PC} = 10.0 Hz, *o*-Ph), 130.0 (d, ⁴J_{PC} = 2.5 Hz, *p*-Ph), 128.5 (s, *p*-C₆H₃), 128.2 (d, ³J_{PC} = 10.2 Hz, *m*-Ph), 124.0 (d, ³J_{PC} = 6.3 Hz, NCH), 123.9 (s, *m*-C₆H₃), 29.3 (s, CH(CH₃)₂), 26.8 (s, CH(CH₃)₂). ³¹P-NMR (101.2, CDCl₃): δ = 8.08 (br d). ¹³C{¹H} NMR (62.9 MHz, CDCl₃): δ = 213.8 (d, ²J_{PC} = 18 Hz, CO) 145.7 (s, *i*-C₆H₃), 139.1 (s, *o*-C₆H₃), 134.5 (d, ²J_{PC} = 10.0 Hz, *o*-Ph), 130.0 (d, ⁴J_{PC} = 2.5 Hz, *p*-Ph), 128.5 (s, *p*-C₆H₃), 128.2 (d, ³J_{PC} = 10.2 Hz, *m*-Ph), 124.0 (d, ³J_{PC} = 6.3 Hz, NCH), 123.9 (s, *m*-C₆H₃), 29.3 (s, CH(CH₃)₂), 26.8 (s, CH(CH₃)₂). ³¹P-NMR (101.2, CDCl₃): δ = 8.08 (br d). ¹³C{¹H} NMR (62.9 MHz, CDCl₃): δ = 213.8 (d, ²J_{PC} = 18 Hz, CO) 145.7 (s, *i*-C₆H₃), 139.1 (s, *o*-C₆H₃), 134.5 (d, ²J_{PC} = 10.0 Hz, *o*-Ph), 130.0 (d, ⁴J_{PC} = 2.5 Hz, *p*-Ph), 128.5 (s, *p*-C₆H₃), 128.2 (d, ³J_{PC} = 10.2 Hz, *m*-Ph), 124.0 (d, ³J_{PC} = 6.3 Hz, NCH), 123.9 (s, *m*-C₆H₃), 29.3 (s, CH(CH₃)₂), 26.8 (s, CH(CH₃)₂). ³¹P-NMR (101.2, CDCl₃): δ = 8.08 (br d). ¹³C{¹H} NMR (62.9 MHz, CDCl₃): δ = 213.8 (d, ²J_{PC} = 18 Hz, CO) 145.7 (s, *i*-C₆H₃), 139.1 (s, *o*-C₆H₃), 134.5 (d, ²J_{PC} = 10.0 Hz, *o*-Ph), 130.0 (d, ⁴J_{PC} = 2.5 Hz, *p*-Ph), 128.5 (s, *p*-C₆H₃), 128.2 (d, ³J_{PC} = 10.2 Hz, *m*-Ph), 124.0 (d, ³J_{PC} = 6.3 Hz, NCH), 123.9 (s, *m*-C₆H₃), 29.3 (s, CH(CH₃)₂), 26.8 (s, CH(CH₃)₂). ³¹P-NMR (101.2, CDCl₃): δ = 8.08 (br d). ¹³C{¹H} NMR (62.9 MHz, CDCl₃): δ = 213.8 (d, ²J_{PC} = 18 Hz, CO) 145.7 (s, *i*-C₆H₃), 139.1 (s, *o*-C₆H₃), 134.5 (d, ²J_{PC} = 10.0 Hz, *o*-Ph), 130.0 (d, ⁴J_{PC} = 2.5 Hz, *p*-Ph), 128.5 (s, *p*-C₆H₃), 128.2 (d, ³J_{PC} = 10.2 Hz, *m*-Ph), 124.0 (d, ³J_{PC} = 6.3 Hz, NCH), 123.9 (s, *m*-C₆H₃), 29.3 (s, CH(CH₃)₂), 26.8 (s, CH(CH₃)₂). ³¹P-NMR (101.2, CDCl₃): δ = 8.08 (br d). ¹³C{¹H} NMR (62.9 MHz, CDCl₃): δ = 213.8 (d, ²J_{PC} = 18 Hz, CO) 145.7 (s, *i*-C₆H₃), 139.1 (s, *o*-C₆H₃), 134.5 (d, ²J_{PC} = 10.0 Hz, *o*-Ph), 130.0 (d, ⁴J_{PC} = 2.5 Hz, *p*-Ph), 128.5 (s, *p*-C₆H₃), 128.2 (d, ³J_{PC} = 10.2 Hz, *m*-Ph), 124.0 (d, ³J_{PC} = 6.3 Hz, NCH), 123.9 (s, *m*-C₆H₃), 29.3 (s, CH(CH₃)₂), 26.8 (s, CH(CH₃)₂). ³¹P-NMR (101.2, CDCl₃): δ = 8.08 (br d). ¹³C{¹H} NMR (62.9 MHz, CDCl₃): δ = 213.8 (d, ²J_{PC} = 18 Hz, CO) 145.7 (s, *i*-C₆H₃), 139.1 (s, *o*-C₆H₃), 134.5 (d, ²J_{PC} = 10.0 Hz, *o*-Ph), 130.0 (d, ⁴J_{PC} = 2.5 Hz, *p*-Ph), 128.5 (s, *p*-C₆H₃), 128.2 (d, ³J_{PC} = 10.2 Hz, *m*-Ph), 124.0 (d, ³J_{PC} = 6.3 Hz, NCH), 123.9 (s, *m*-C₆H₃), 29.3 (s, CH(CH₃)₂), 26.8 (s, CH(CH₃)₂). ³¹P-NMR (101.2, CDCl₃): δ = 8.08 (br d). ¹³C{¹H} NMR (62.9 MHz, CDCl₃): δ = 213.8 (d, ²J_{PC} = 18 Hz, CO) 145.7 (s, *i*-C₆H₃), 139.1 (s, *o*-C₆H₃), 134.5 (d, ²J_{PC} = 10.0 Hz, *o*-Ph), 130.0 (d, ⁴J_{PC} = 2.5 Hz, *p*-Ph), 128.5 (s, *p*-C₆H₃), 128.2 (d, ³J_{PC} = 10.2 Hz, *m*-Ph), 124.0 (d, ³J_{PC} = 6.3 Hz, NCH), 123.9 (s, *m*-C₆H₃), 29.3 (s, CH(CH₃)₂), 26.8 (s, CH(CH₃)₂). ³¹P-NMR (101.2, CDCl₃): δ = 8.08 (br d). ¹³C{¹H} NMR (62.9 MHz, CDCl₃): δ = 213.8 (d, ²J_{PC} = 18 Hz, CO) 145.7 (s, *i*-C₆H₃), 139.1 (s, *o*-C₆H₃), 134.5 (d, ²J_{PC} = 10.0 Hz, *o*-Ph), 130.0 (d, ⁴J_{PC} = 2.5 Hz, *p*-Ph), 128.5 (s, *p*-C₆H₃), 128.2 (d, ³J_{PC} = 10.2 Hz, *m*-Ph), 124.0 (d, ³J_{PC} = 6.3 Hz, NCH), 123.9 (s, *m*-C₆H₃), 29.3 (s, CH(CH₃)₂), 26.

Synthesis of 11 via Pd-catalyzed amination of bromobenzene with 2,6-diisopropylaniline

(a) **With conventional heating:** A 100 mL reaction vessel was charged with Pd(OAc)₂ (36 mg, 0.16 mmol, 2 mol-%), a phosphine (137 mg of **5a** or 63 mg of PPh₃, 0.24 mmol, 3 mol-%), and NaOtBu (1.15 g, 12 mmol). Toluene (30 mL) was added and the mixture refluxed for 10 min to yield a yellowish orange solution. Bromobenzene (1.29 g, 0.86 mL, 8.22 mmol) and 2,6-diisopropylaniline (1.77 g, 1.82 mL, 10 mmol) were added. The solution was then refluxed under stirring for 2 h during which time a greyish precipitate formed. The suspension was allowed to cool to ambient temperature. An aliquot (0.10 mL) of the supernatant liquid was withdrawn, quenched by addition of CDCl₃ (0.50 mL), and the resulting solution analyzed by recording a ¹H NMR spectrum. Deconvolution of the CH₂(iPr) region allowed to determine the molar amount of product in relation to all iPr-containing species in the solution. This value was then used to calculate the degree of conversion. The bulk reaction mixture of the run conducted with **5a** was quenched by addition of saturated aqueous NH₄Cl (20 mL). EtOAc (30 mL) was added, the organic layer of the resulting biphasic mixture separated, and the aqueous phase washed with EtOAc (3 x 10 mL). The combined organic phases were dried with Na₂SO₄, filtered, and evaporated to dryness. The remaining red oil was purified by chromatography (silica, eluent 120 mL hexane/EtOAc 30:1). Evaporation of the eluate to dryness afforded 1.49 g (5.9 mmol, 72% yield) of **11** as a colorless, crystalline material. – ¹H NMR (250 MHz, CDCl₃): δ = 7.25–7.12 (m, 4 H, o/m-Ph), 7.06 (t, 1 H, ³J_{HH} = 7.7 Hz, p-C₆H₃), 6.63 (t, 1 H, ³J_{HH} = 7.3 Hz, p-Ph), 6.40 (d, 2 H, ³J_{HH} = 7.7 Hz, m-C₆H₃), 5.04 (s, 1 H, NH), 3.13 (sept, 2 H, ³J_{HH} = 6.9 Hz, CH(CH₃)₂), 1.07 (d, 12 H, ³J_{HH} = 6.9 Hz, CH(CH₃)₂). – Anal. for C₁₈H₂₃N (253.39 g mol⁻¹): calcd. C 85.32 H 9.15 N 5.53%; found C 85.31 H 9.23 N 5.44%.

For kinetic studies, the preparation of the reaction mixture and the addition of reactants were carried out as described, except that only 0.2 mol-% of Pd(OAc)₂ (3.7 mg, 16 μmol) and 0.3 mol-% of phosphine (14.1 mg of **5a** or 6.3 mg of PPh₃, 25 μmol) were employed. After all reagents had been added, an aliquot of the reaction mixture was withdrawn and subjected to ¹H NMR analysis as described above. The mixture was then refluxed for 2 h (reaction with **5a**) or 3 h (reaction with PPh₃). Aliquots (0.10 mL) were withdrawn every five min during the first 90 min. In the reaction with PPh₃, additional samples were drawn after 120, 150, and 180 min. Analysis of all samples was carried out as described; the results are included in the supporting information. No work-up was attempted.

(b) **Under microwave irradiation:** A microwave reaction vessel (volume 30 mL) was charged with bromobenzene (2.83 g, 1.89 mL, 18 mmol), 2,6-diisopropylaniline (3.55 g, 3.64 mL, 20 mmol), NaOtBu (2.00 g, 21 mmol), Pd(OAc)₂ (81 mg, 0.36 mmol, 2 mol-%), ligand **5a** (206 mg, 0.36 mmol, 3 mol-%), and toluene (10 mL). The vessel was placed into the microwave reactor, heated to 200 °C and held at this temperature for 10 min before being cooled down to ambient temperature. The reaction mixture was stirred during the whole procedure at a rate of 1200 rpm. The greyish precipitate was allowed to settle down and the mixture then analyzed as described under (a). No work-up was attempted.

Synthesis of 12: A 100 mL reaction vessel was charged with Pd(OAc)₂ (13 mg, 0.16 mmol, 0.7 mol-%), **5a** (50 mg, 0.24 mmol, 1.1 mol-%), NaOtBu (419 mg, 4.37 mmol), amine **11** (880 mg, 3.47 mmol), and toluene (11 mL). The mixture was refluxed for 10 min, bromobenzene (453 mg, 0.31 mL, 2.88 mmol) was added, and the reaction mixture refluxed for 24 h. Stirring was maintained during the whole procedure. Further analysis and work-up was carried out as described above. The crude product obtained after extraction was recrystallized from MeOH to afford 742 mg (2.25 mmol, 65%) of **12** as colorless crystalline material. – ¹H NMR (250 MHz, CDCl₃): δ = 7.30 (m, 1 H, p-C₆H₃), 7.17 (m, 2 H, m-C₆H₃), 7.10 (m, 4 H, m-Ph), 6.93 (m, 4 H, o-Ph), 6.79 (m, 2 H, p-Ph), 3.08

(sept, 2 H, ³J_{HH} = 6.8 Hz, CH(CH₃)₂), 0.85 (d, 12 H, ³J_{HH} = 6.8 Hz, CH(CH₃)₂).

Synthesis of phenyl piperidine: Reaction and work-up were carried out by analogy to the synthesis of **10** using 36 mg (0.16 mmol, 2 mol-%) of Pd(OAc)₂, 137 mg (0.24 mmol, 3 mol-%) of **5a**, 1.15 g (12 mmol) of NaOtBu, 851 mg (0.95 mL, 10 mmol) piperidine, and 1.29 g (0.86 mL, 8.22 mmol) bromobenzene in 30 mL toluene. The crude oil obtained after the extraction procedure solidified upon overnight storage at -15 °C. The product was identified by ¹H NMR; no yield was determined. ¹H NMR (250 MHz, CDCl₃): δ = 7.15 (m, 2 H, m-Ph), 6.90 (d, 2 H, ³J_{HH} = 8.0 Hz, o-Ph), 6.75 (t, 1 H, ³J_{HH} = 7.3 Hz, 1 H, p-Ph), 3.08 (t, 4 H, ³J_{HH} = 5.3 Hz, NCH₂), 1.65 (m, 4 H, NCCH₂), 1.52 (m, 2 H, NCCCH₂).

Computational studies: RI-DFT calculations were carried out on the bwForCluster Justus with the TURBOMOLE [31] program suite (version 7.2.2017 [32]). Energy optimization of molecular structures was carried out using the BP86 functional with a def2-svp basis set [33] and Grimme's D3BJ formalism [34] to include dispersion effects. The buried volume of ligands was calculated using the SambVca2.0 online tool [35] with the default settings provided.

Crystal structure determinations. Diffraction studies were carried out using a Bruker diffractometer equipped with a Kappa Apex II Duo CCD-detector and a KRYO-FLEX cooling device with Mo-K_α radiation (λ = 0.71073 Å) at T = 100(2) K for **7b** and T = 130(2) K for **6b**, **8b**. The structures were solved by direct methods (SHELXS-97[36]) and refined with a full-matrix least-squares scheme on F² (SHELXL-2014[36]). Semi-empirical absorption corrections were applied for all structures. Non-hydrogen atoms were refined anisotropically except when disordered, the hydrogen atoms at phosphorus isotropically, and all other hydrogen atoms with a riding model. One iPr-group in **8b** is disordered over two positions. Disordered atoms were refined isotropically and with restraints. CCDC-1866063 (**6b**), CCDC-1866064 (**7b**), and CCDC-1866065 (**8b**) contain the supplementary crystallographic data for this paper. This data can be obtained free of charge from the Cambridge Crystallographic Data Centre via www.ccdc.cam.ac.uk/data_request/cif.

Acknowledgments

The computational studies were supported by the bwHPC initiative and the bwHPC-C5 project provided through the associated compute services of the JUSTUS HPC facility at the University of Ulm. bwHPC and bwHPC-C5 (<http://www.bwhpc-c5.de>) are funded by the state of Baden-Württemberg and the DFG (grant no. INST 40/467-1 FUGG). We further thank B. Förtsch for elemental analyses and Dr. W. Frey (Institute of Organic Chemistry, University of Stuttgart) for the collection of X-ray data sets.

Keywords: Phosphane ligands • Ligand effects • Cross-coupling • Palladium • Boranes

- [1] C. A. Tolman, *Chem. Rev.* **1977**, *77*, 313–348.
- [2] R. J. Lundgren, M. Stradiotto, *Aldrichim. Acta* **2012**, *45*, 59–65.
- [3] a) A. S. Guram, R. A. Rennels, S. L. Buchwald, *Angew. Chem. Int. Ed.* **1995**, *34*, 1348–1350; b) J. Louie, J. F. Hartwig, *Tetrahedron Lett.* **1995**, *36*, 3609–3612; c) S. L. Buchwald, A. S. Guram, U.S. Patent 5,576,460, **1996**.

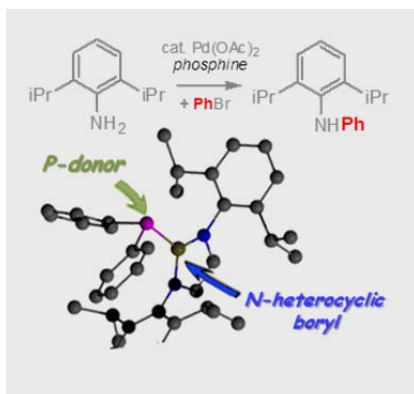
- [4] For recent reviews, see: a) D. S. Surry, S. L. Buchwald, *Chem. Sci.* **2011**, *2*, 27–50; b) J. F. Hartwig, *Acc. Chem. Res.* **2008**, *41*, 1534–1544; c) S. L. Buchwald, C. Mauger, G. Mignani, U. Scholz, *Adv. Synth. Catal.* **2006**, *348*, 23–29; d) B.; Schlummer, U. Scholz, *Adv. Synth. Catal.* **2004**, *346*, 1599–1626; e) A. S. Guram, *Org. Process Res. Dev.* **2016**, *20*, 1754–1764.
- [5] C. A. Fleckenstein, H. Plenio, *Chem. Soc. Rev.* **2010**, *39*, 694–711.
- [6] A. M. Spokoiny, C. D. Lewis, G. Teverovskiy, S. L. Buchwald, *Organometallics* **2012**, *31*, 8478–8481.
- [7] D. A. Hoic, W. M. Davis, G. C. Fu *J. Am. Chem. Soc.* **1996**, *118*, 8176–8177.
- [8] a) N. Kuhn, R. Fawzi, M. Steimann, J. Wiethoff, *Chem. Ber.* **1996**, *129*, 479–482; b) N. Kuhn, H. Kotowski, J. Wiethoff, *Phosphorus, Sulfur, Silicon Rel. El.* **1998**, *133*, 237–244.
- [9] M. A. Wünsche, P. Mehlmann, T. Witteler, F. Buß, P. Rathmann, F. Dielmann, *Angew. Chem. Int. Ed.* **2015**, *54*, 11857–11860.
- [10] A related, although not heteroatom-based, substituent that has recently been introduced into phosphine chemistry is the N-heterocyclic olefin unit; see: a) N. R. Paisley, M. W. Lui, R. McDonald, M. J. Ferguson, E. Rivard, *Dalton Trans.* **2016**, *45*, 9860–9870; b) Review: M. M. D. Roy, E. Rivard, *Acc. Chem. Res.* **2017**, *50*, 2017–2025.
- [11] The chemistry of imidazolin-2-ylideneimino-substituted main-group element compounds (including phosphines) has recently been reviewed: T. Ochiai, D. Franz, S. Inoue, *Chem. Soc. Rev.* **2016**, *45*, 6327–6344.
- [12] F. Buß, P. Mehlmann, C. Mück-Lichtenfeld, K. Bergander, F. Dielmann, *J. Am. Chem. Soc.*, **2016**, *138*, 1840–1843.
- [13] a) J. A. Bailey, M. Ploeger, P. G. Pringle, *Inorg. Chem.* **2014**, *53*, 7763–7769; J. A. Bailey, M.F. Haddow, P.G. Pringle, *Chem. Commun.* **2014**, *50*, 1432–1434.
- [14] M. Kaaz, J. Bender, D. Förster, W. Frey, M. Nieger, D. Gudat, *Dalton Trans.* **2014**, *43*, 680–689.
- [15] M. Kaaz, C. Bäucker, M. Deimling, S. König, S. H. Schlindwein, J. Bender, M. Nieger, D. Gudat, *Eur. J. Inorg. Chem.* **2017**, 4525–4532.
- [16] A. Amgoune, S. Ladeira, K. Miqueu, D. Bourissou, *J. Am. Chem. Soc.* **2012**, *134*, 6560–6563.
- [17] Result of a query in the CSD database for complexes $[(R_3P)Fe(CO)_4]$ with R = non-metal based substituent.
- [18] Review: a) N. Fey, A. G. Orpen, J. N. Harvey, *Coord. Chem. Rev.* **2009**, *253*, 704–722; b) O. Köhl, *Coord. Chem. Rev.* **2005**, *249*, 693–704.
- [19] Further studies revealed that the complexes decayed during attempts to their crystallization by release of CO and reaction with cod under regeneration of complexes $[RhCl(NHB\text{-phosphine})(cod)]$ and formation of further trace products which were not identifiable. The changes were reversible when the solution was once again saturated with CO.
- [20] T. Dröge, F. Glorius, *Angew. Chem. Int. Ed.* **2010**, *49*, 6940–6952.
- [21] J. D. Cotton, M. M. Kroes, R. D. Markwell, E. A. Miles, *J. Organomet. Chem.* **1990**, *388*, 133–142.
- [22] T. Bartik, T. Himmler, H.-G. Schulte, K. Seevogel, *J. Organomet. Chem.* **1984**, *272*, 29–41.
- [23] K. A. Buntten, L. Chen, A. L. Fernandez, A. J. Poë, *Coord. Chem. Rev.* **2002**, *233–234*, 41–51.
- [24] a) A. C. Hillier, W. J. Sommer, B. S. Yong, J. L. Petersen, L. Cavallo, S. P. Nolan, *Organometallics* **2003**, *22*, 4322–4326; b) A. Poater, B. Cosenza, A. Correa, S. Giudice, F. Ragone, V. Scarano, L. Cavallo, *Eur. J. Inorg. Chem.* **2009**, 1759–1766.
- [25] R. Martin, S. L. Buchwald, *Acc. Chem. Res.* **2008**, *41*, 1461–1473.
- [26] C. Singh, J. Rathod, V. Jha, A. Panossian, P. Kumar, F. R. Leroux, *Eur. J. Org. Chem.* **2015**, 6515–6525.
- [27] Several alternative protocols for the synthesis of **10** via the Buchwald-Hartwig approach have been also reported: a) Maxim A.; Topchiy, Pavel B.; Dzhevakov, Margarita S.; Rubina, Oleg S.; Morozov, Andrey F.; Asachenko, Mikhail S. Nechaev, *Eur. J. Org. Chem.* **2016**, 1908–1914; b) Y. Chen, A. Turlik, T. R. Newhouse, *J. Am. Chem. Soc.* **2016**, *138*, 1166–1169; c) D. Mendoza-Espinosa, R. Gonzalez-Olvera, C. Osornio, G. E. Negron-Silva, A. Alvarez-Hernandez, C. I. Bautista-Hernandez, O. R. Suarez-Castillo, *J. Organomet. Chem.* **2016**, *803*, 142–149; d) J. P. Tassone, G. J. Spivak, *J. Organomet. Chem.* **2017**, *841*, 57–61; e) D. C. Samblanet, J. A. R. Schmidt, *J. Organomet. Chem.* **2012**, *720*, 7–18.
- [28] C. O. Kappe, *Angew. Chem. Int. Ed.* **2004**, *43*, 6250–6284.
- [29] a) L. Shi, M. Wang, C.-A. Fan, F.-M. Zhang, Y.-Q. Tu, *Org. Lett.* **2003**, *5*, 3515–3517; b) X. Meng, Z. Cai, S. Xiao, W. Zhou, J. Fluorine Chem. **2013**, *146*, 70–75; c) R. Singh, B. K. Allam, D. S. Raghuvanshi, K. N. Singh, *Tetrahedron* **2013**, *69*, 1038–1042.
- [30] J. A. Bailey, P. G. Pringle, *Coord. Chem. Rev.* **2015**, 297–298, 77–90.
- [31] R. Ahlrichs, M. Bär, M. Häser, H. Horn, C. Kölmel, *Chem. Phys. Lett.* **1989**, *162*, 165–169.
- [32] TURBOMOLE V7.2 2017, a development of University of Karlsruhe and Forschungszentrum Karlsruhe GmbH, 1989–2007, TURBOMOLE GmbH, since 2007; available from <http://www.turbomole.com>.
- [33] F. Weigend, R. Ahlrichs, *Phys. Chem. Chem. Phys.* **2005**, *7*, 3297–3305.
- [34] S. Grimme, S. Ehrlich, L. Goerigk, *J. Comp. Chem.* **2011**, *32*, 1456–1465.
- [35] L. Falivene, R. Credendino, A. Poater, A. Petta, L. Serra, R. Oliva, V. Scarano, L. Cavallo, *Organometallics* **2016**, *35*, 2286–2293.
- [36] G. M. Sheldrick, *Acta Cryst.* **2008**, *A64*, 112–122

Entry for the Table of Contents (Please choose one layout)

Layout 1:

FULL PAPER

Phosphines with an N-heterocyclic boryl substituent at phosphorus behave as strongly electron releasing ligands that may impart despite their conformational flexibility sizable steric shielding to a transition metal atom. This makes them suitable candidates for application as ligands in cross-coupling chemistry.



Electron rich phosphines

M. Kaaz, R. J. C. Locke, L. Merz, M. Benedikter, S. König, J. Bender, S. H. Schlindwein, M. Nieger and D. Gudat*

Page No. – Page No.

Phosphines with N-heterocyclic Boryl-substituents: Ligands for Coordination Chemistry and Catalysis